INFRASTRUCTURE SOLUTIONS

BEHAVIOR OF CONCRETE SLABS REINFORCED WITH FIBERGLASS REBAR UNDER RESTRAINED SHRINKAGE

Antonio Mudadu, Giuseppe Tiberti, Bryan Barragan and Giovanni Plizzari

BIOGRAPHY

Antonio Mudadu, Ph.D., Postdoctoral fellow at the Department of Civil, Environmental, Architectural Engineering and Mathematics, University of Brescia, Italy. antonio.mudadu@unibs.it, Tel: +39 0303715965.

Giuseppe Tiberti, Associate Professor of Structural Engineering at the Department of Civil Engineering, Architecture, Land, Environment and of Mathematics, University of Brescia, Italy. giuseppe.tiberti@unibs.it, Tel: +39 0303711287.

Bryan E. Barragan, PhD, Global Technical Leader, Owens Corning Infrastructure Solutions. Chambéry, France. bryan.barragan@owenscorning.com

Giovanni A. Plizzari, Professor of Structural Engineering at the Department of Civil Engineering, Architecture, Land, Environment and of Mathematics, University of Brescia, Italy. giovanni.plizzari@unibs.it, Tel: +39 0303711285.

ABSTRACT

The present paper presents an experimental study proving the effectiveness of Glass Fiber Reinforced Polymer (GFRP) rebar, also known as fiberglass rebar, rebars as shrinkage reinforcement for slabs-on-ground, when compared to a traditional steel rebar solution. Unidimensional slabs reinforced with steel and fiberglass rebars have been cast and restrained to steel frames providing high degree of restrain to shrinkage deformations, thus providing conditions to produce shrinkage cracking in the elements. In this way, the effectiveness of the different solutions can be evaluated.

Displacement transducers were placed on the surface of the slabs to continuously monitor longitudinal displacements along time. Moreover, the number of cracks was visually quantified, and its opening measured with an electronic microscope.

Other specimens were also made to measure compressive strength and the free shrinkage of concrete. Ambient temperature and relative humidity were continuously measured over the whole tests.

Results show that fiberglass rebars can be an effective solution to control shrinkage cracking in slabs on ground. More specifically, 10 mm (#3) and 13 mm (#4) fiberglass rebars have both shown a better crack control capacity than 12 mm (#4) steel rebars.

Keywords: Glass fiber reinforced polymer reinforcement, slabs-on-ground, restrained shrinkage cracking.

1. INTRODUCTION

Mainly due to its practical advantages related to its lightweight leading to an easier and faster construction, and consequent labor savings, fiberglass rebar reinforcement is increasingly becoming an alternative choice for concrete flatwork projects in North America.

However, while fiberglass rebar has shown to work equally than steel reinforcement, there has been little, if any, research work dealing specifically with this application of fiberglass reinforcement. Until few years ago, fiberglass rebar reinforcement has been mainly used for its intrinsic corrosion resistance and extension of the life span of concrete structures, and/or due to its electromagnetic transparency. This work addresses an experimental study proving the effectiveness of fiberglass rebar as shrinkage reinforcement for slabs-on-ground, when compared to a traditional steel rebar solution. Unidimensional slabs reinforced with steel and fiberglass rebars have been cast inside steel frames providing high degree of restrain to shrinkage deformations, i.e. providing conditions to produce shrinkage cracking in the elements. In this way, the effectiveness of the different solutions can be evaluated.

2. EXPERIMENTAL PROGRAM

Three 10 ft long x 3.3 ft wide x 6 in. thick (3.0m x 1.0m x 0.15m) slabs were cast with a 3500 psi (25 MPa) concrete inside a rigid steel frame **(Figure 1 and Figure 2)**. To restrain the slab shrinkage and force cracking, the concrete was anchored at the ends by threaded rods, and isolated from the lateral mold and bottom surfaces by a plastic sheet to prevent friction along those surfaces **(Figure 2a)**. The rebar reinforcement was placed at the upper third of the slabs, kept in place by spacers **(Figure 2a)**. Each slab had a different reinforcement solution, as shown in **Table 1**.

TABLE 1. SLAB REINFORCEMENT

SLAB	REINFORCEMENT	BAR SIZE AND SPACING	
		IMPERIAL	SI
1	Steel rebar	2#4@18"	2x12mm@450mm
2	Fiberglass rebar	2#4@18"	2x12mm@450mm
3	Fiberglass rebar	2#3@18"	2x10mm@450mm

The formworks were filled by means of a bucket. Minor compaction was manually applied with a ruler on the top of the slab, which was finally troweled to achieve a smooth finishing. To simulate a more demanding situation (which can take place when not following best practices), no curing was implemented on the surface of the slab; only the bleeding water kept the surface wet during the first hours after concrete pouring.

Just after casting displacement transducers were placed on the surface of the slabs to continuously monitor longitudinal displacements along time **(Figure 2)**.

Ambient temperature and relative humidity were measured continuously along the duration of the tests. After the surface of the slab was sufficiently hard and dry, the slabs were painted with a white water-based paint to better observe crack onset and development; crack opening was measured with an electronic microscope (Dino-Lite AM4113T) with a x200 magnification. Specific measuring points were defined along the cracks to track the evolution of the cracks along time, since the crack width may not be uniform along its length.

FIGURE 1 – Test set-up and instrumentation layout for shrinkage test (a) steel frame, (b) concrete slab and layout instrumentation (dimentions in mm)

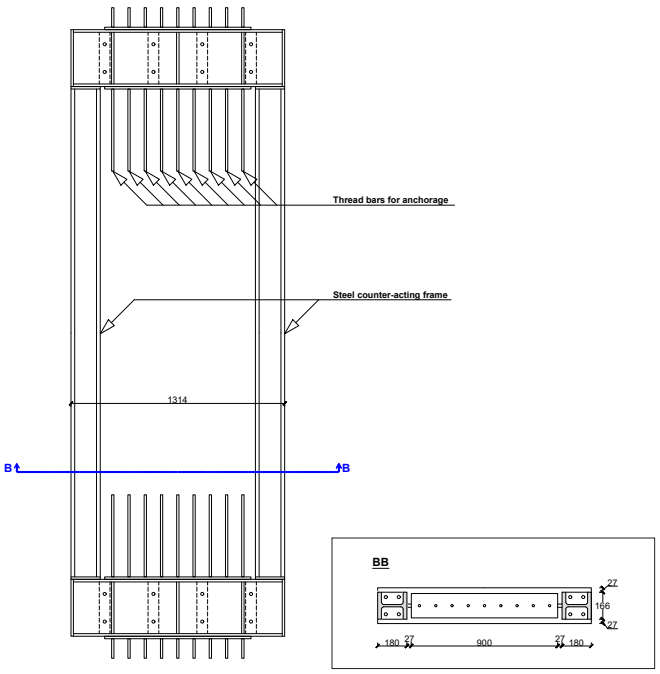

(A)

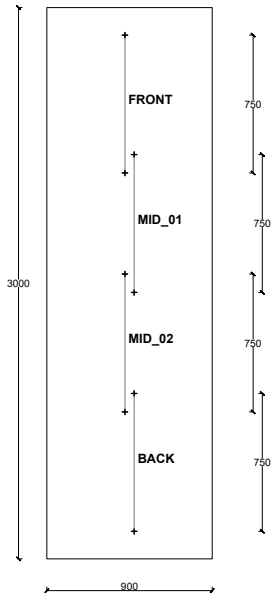

(B)

FIGURE 2 – Test setup details. a) mold setup including anti-friction plastic films, "snake"-type spacers or chairs, and threaded anchorage rods, b) view of specimens just after casting, c) LDT transducers mounted on the painted surface

(A)

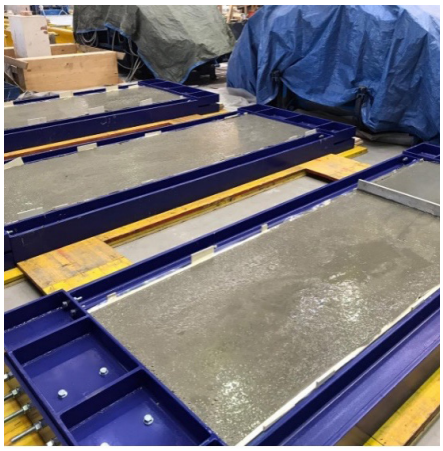

(B)

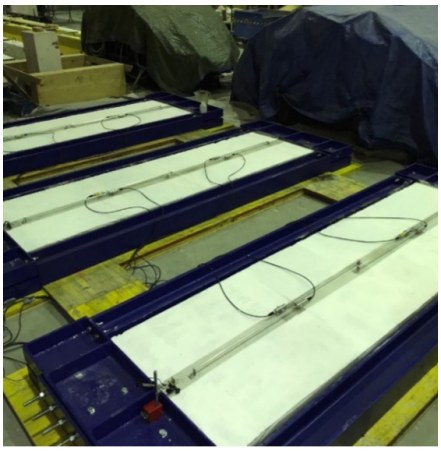

(C)

2.1 MATERIALS AND SPECIMENS GEOMETRY

Table 2 summarizes the material properties and rebar diameter (both for steel and fiberglass rebar) used in the study. Steel rebars were a standard grade B 400 S while fiberglass rebar used were PINKBAR® Fiberglas™ Rebar by Owens Corning Infrastructure Solutions (OCIS) for flatwork applications. The C20/25 concrete typically used in flatwork applications, was supplied by a local ready-mix concrete company.

TABLE 2. MATERIAL PROPERTIES

REBAR	NOMINAL DIAMETER (MM)	GUARANTEED TENSILE STRENGTH+ (MPA)	MEAN E-MODULUS+ (GPA)	GUARANTEED BOND STRENGTH+ (MPA)
Steel rebar	12	400*	210	
Fiberglass rebar	9.5	981	46	13.7
Fiberglass rebar	12.7	910	46	13.7

Compressive strength was measured on 150 mm (6 inch) cubes, at 3, 7, 14 and 28 days. **Figure 3** shows its evolution along time. The average compressive strength at 28 days was 31 MPa (4496 psi).

FIGURE 3 – Compressive strength vs. time based on cubes 150x150x150mm^3

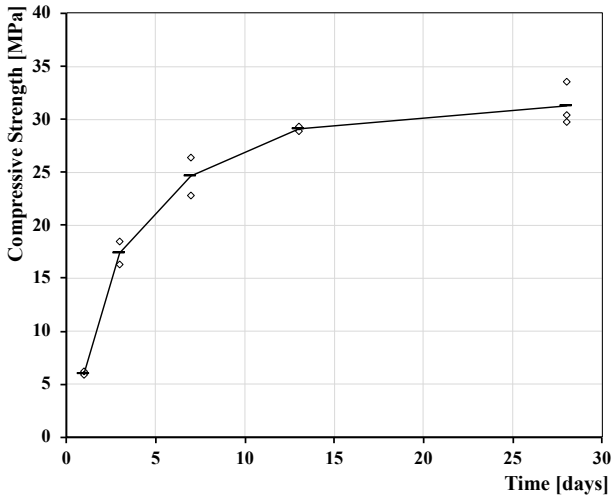

Free shrinkage of concrete was measured on three sample prisms of 75x75x250 mm (3x3x10 in), according to EN 12390-16 [ ], in order to fully retrieve the shrinkage evolution over the time as well as the maximum shrinkage developed by the concrete **(Figure 4)**. Both the device adopted for this test and the prisms were subjected to the same environmental condition than the slabs (free shrinkage were prisms kept next to the slabs).

Appendix A 1 lists the time between casting and measurement, environmental conditions at the time of data acquisition, the shrinkage values measured on each sample, and the mean value from the 3 specimens.

The shrinkage measures reported in **Appendix A 1** are plotted in **Figure 4**, where the shrinkage development over time can be observed. The graph reports the evolution of the individual specimens as well as the mean value. As it can be observed, a rapid shrinkage increase takes place until approx. 20 days after casting, beyond which the shrinkage rate decreases until reaching an almost asymptotic behavior at approx. 60 days. At about 90 days, the average total shrinkage recorded was 665 microstrains, which is in the expected level for the concrete class used in these tests.

FIGURE 4 – Shrinkage specimen length change vs. Time and test setup

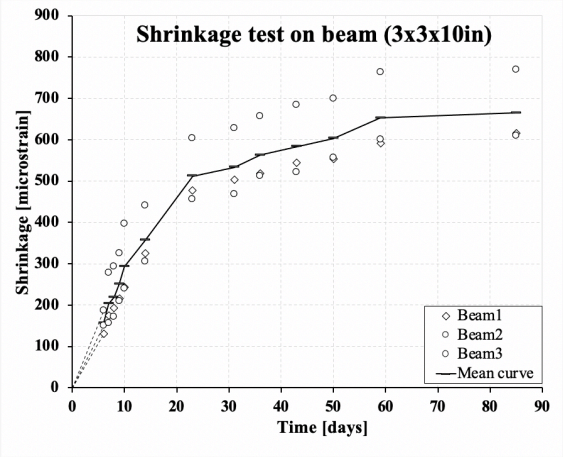

2.2 ENVIRONMENTAL CONDITION

Figure 5a and b show the variations of temperature and humidity along the time of the tests. As it can be observed, the average temperature was 18˚C (64˚F) with an overall variation of ± 6˚C (43˚F); average relative humidity was 37%, ranging from 16% to 58%. Because of slabs were located inside the laboratory, they were subjected to small variations in terms of temperature; in fact, the daily temperature variation was around 3-5°C (5-10°F).

FIGURE 5 – Temperature (a) and Relative Humidity (b) of the environment vs. Time

(A)

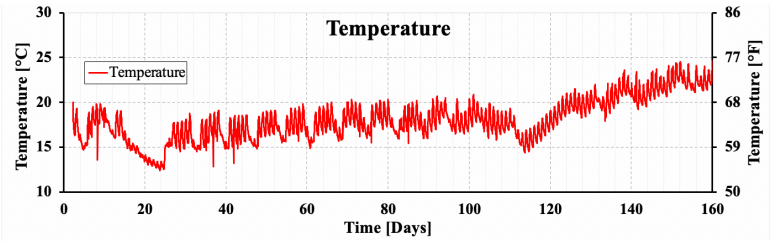

(B)

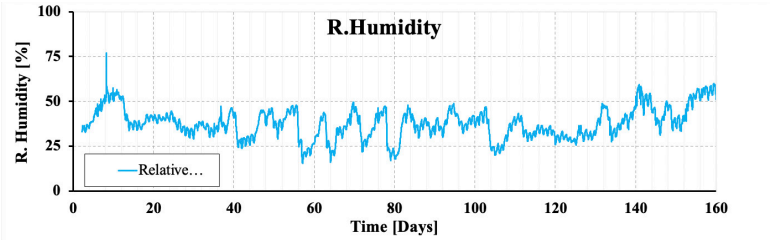

3. RESULTS AND DISCUSSION

The readings over the time obtained from the linear displacement transducers (LDTs) placed on the surface of the slab are reported in **Figure 6a, b, and c** for steel rebar Φ12@45cm (#4@18"), fiberglass rebar Φ13@45cm (#4@18") and fiberglass rebar Φ10@45cm (#3@18"), respectively. Nomenclature adopted for the curves refers to the LDT location on the slab, in accordance with **Figure 1b**. "FRONT" and "BACK" LDT were mounted in proximity of the anchorage in order to evaluate this disturbed region; whereas "MID_01" and "MID_02" were designed to detect the central region in which the cracks were expected.

As shown in **Figure 1b**, LDT transducers have a measuring length equal to 750 mm (29.5 in). Because of the long measuring span, readings are considerably affected from elastic deformation of the undamaged concrete; hence these transducers are not able to detect micro-cracking on the surface of the slab. However, these LDTs do register along the total length of the slab the occurrence of any macro crack and its evolution. Given that these tests ran along the year 2020, the LDTs were of paramount importance for monitoring the entire shrinkage development along the slabs even when the laboratory was not accessible.

As it can be observed from **Figure 6**, in general terms a non-linear elastic behavior arises at approx. 10 days after casting. Due to temperature and relative humidity variations, slight jumps can be noted in all the slabs and continues for the entire duration of the tests for slabs reinforced with fiberglass rebar.

After approximately 115 days of exposition, a significant temperature increase and a relative humidity decrease occurred **(see Figure 5)**, leading to subsequent displacement increases in the three slabs **(see Figure 6)**.

In the case of the steel rebar reinforced slab, a macro-crack suddenly occurred after 126 days of casting **(see Figure 6a)**.
The LDTs show displacement increases in slabs reinforced with fiberglass rebars as well, but such increase is absorbed and distributed across the micro-cracks (see below) instead of concentrating in 1 single macro-crack.

FIGURE 6 – Displacements vs. Time detected from LDTs transducers mounted on slab surface; a) steel rebar Φ12@45cm [#4@18"] b) fiberglass rebar Φ13@45cm [#4@18"] c) fiberglass rebar Φ10@45cm [#3@18"]

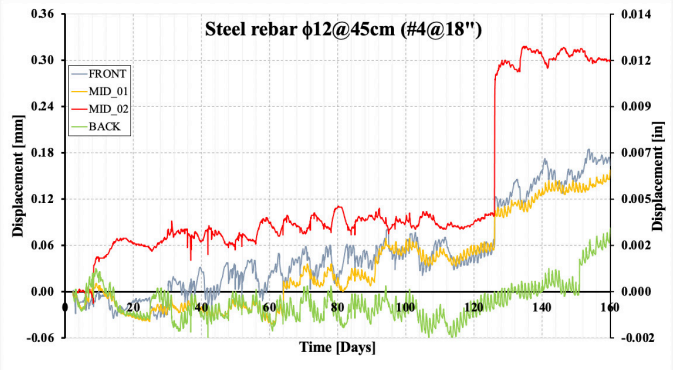

(A)

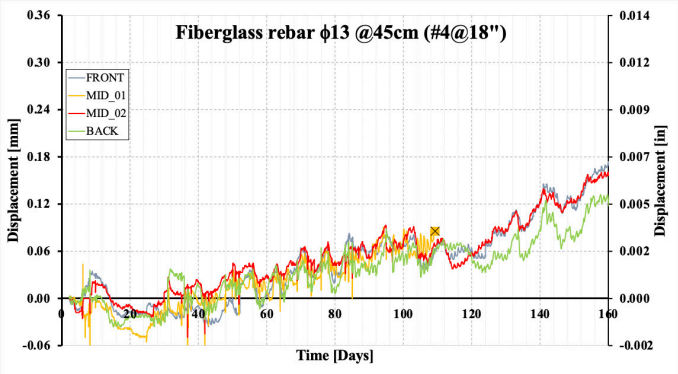

(B)

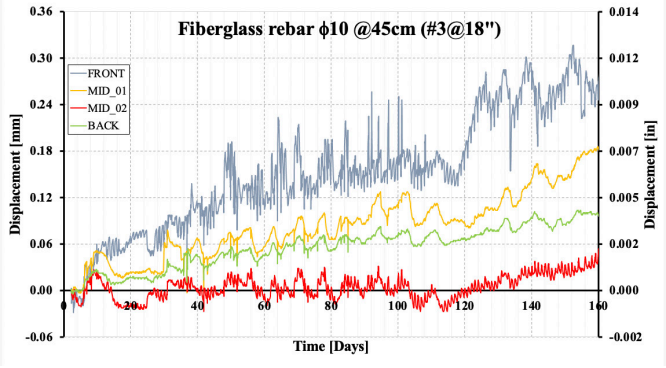

(C)

While the understanding of the different responses from steel and fiberglass rebar reinforced slabs is out of the scope of this limited study, a key and favorable influence of the fiberglass rebar bond and/or modulus of elasticity, may be hypothesized.

Once micro-cracks became visible on the slabs surfaces, an accurate mapping of the crack pattern was carried out starting at 31 days after casting, measuring the crack length and crack width by means of an electronic microscope Dino-Lite AM4113T **(Figure 7)**. **Figure 8** represents the final crack pattern retrieved through this visual inspection.

All slabs exhibit similar micro-crack patterns in the middle half of the slab, where higher stresses develop. As expected, due to the shrinkage deformation, these cracks arose mainly along the transversal direction.

FIGURE 7 – Crack pattern evaluation by means of an electronic microscope Dino-Lite AM4113T (a); Dino-Lite AM4113T detail (b).

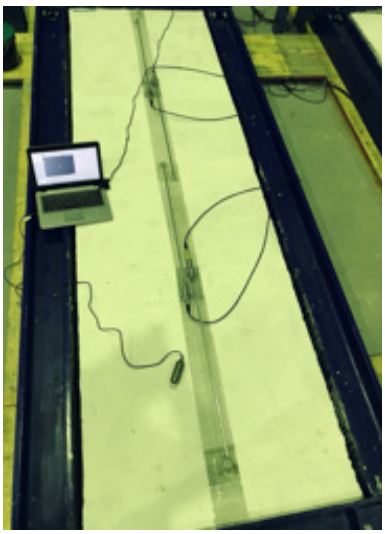

(A)

(B)

Noticeably, the slab reinforced with Fiberglass #3/Φ10 mm shows a larger number of micro-cracks (not visible to the naked-eye). Given the mainly random pattern of these micro-cracks and the fact that they are located rather out of the central half of the slab (area of lower shrinkage stresses), it is more probable that these are not cracks caused by the restrained shrinkage conditions but actually crazing cracks caused by a soft air flow from an outlet of the laboratory's heating system located high on the wall of the laboratory, approx. 3 meters above that slab.

Comparing slabs including steel and fiberglass rebar #4/Φ13, **Figures 8a and 8b**, respectively, a larger number of micro-cracks are observed in the later **(Figure 8b)**.

As mentioned, once the micro-cracks occurred and the entire crack pattern was defined, the width of selected reference cracks was tracked along time by means of a digital microscope. To obtain the proper behavior of the crack growth along time, exact measurement points were respected in each selected crack; i.e. the microscope was placed exactly in the same position each time a measure was taken on the selected crack. Obviously, the number of reference cracks was enlarged if new relevant cracks appeared.

As it can be seen in **Figure 9**, seven, six, and eleven reference cracks were identified in slabs reinforced with #4/12 mm steel rebar, #4/13 mm fiberglass rebar, and #3/10 mm fiberglass rebar, respectively; the bar graphs show the evolution of each selected crack over the time for each slab.

Appendix A 2 summarizes the data for the three slabs, where crack widths measures over time are listed together with the respective mean and maximum values.

As it can be observed, the micro-crack widths slowly increase up to 90 days in all the slabs, after which the opening rate significantly decreases or stops. All reference cracks in fiberglass-reinforced slabs were micro-cracks with openings well below 0.1 mm. The same behavior was observed in the case of steel-reinforced slabs until a macro-crack appeared in this slab at the age of 126 days, reaching an opening above 0.65mm (0,025") at 209 days.

FIGURE 8 – Crack pattern after 209 days
Micro cracks (————), macro cracks (————) and reference crack location (•)
Steel #4 /Φ12 (a), Fiberglass #4 / Φ13 (b) and Fiberglass #3 / Φ10 (c).

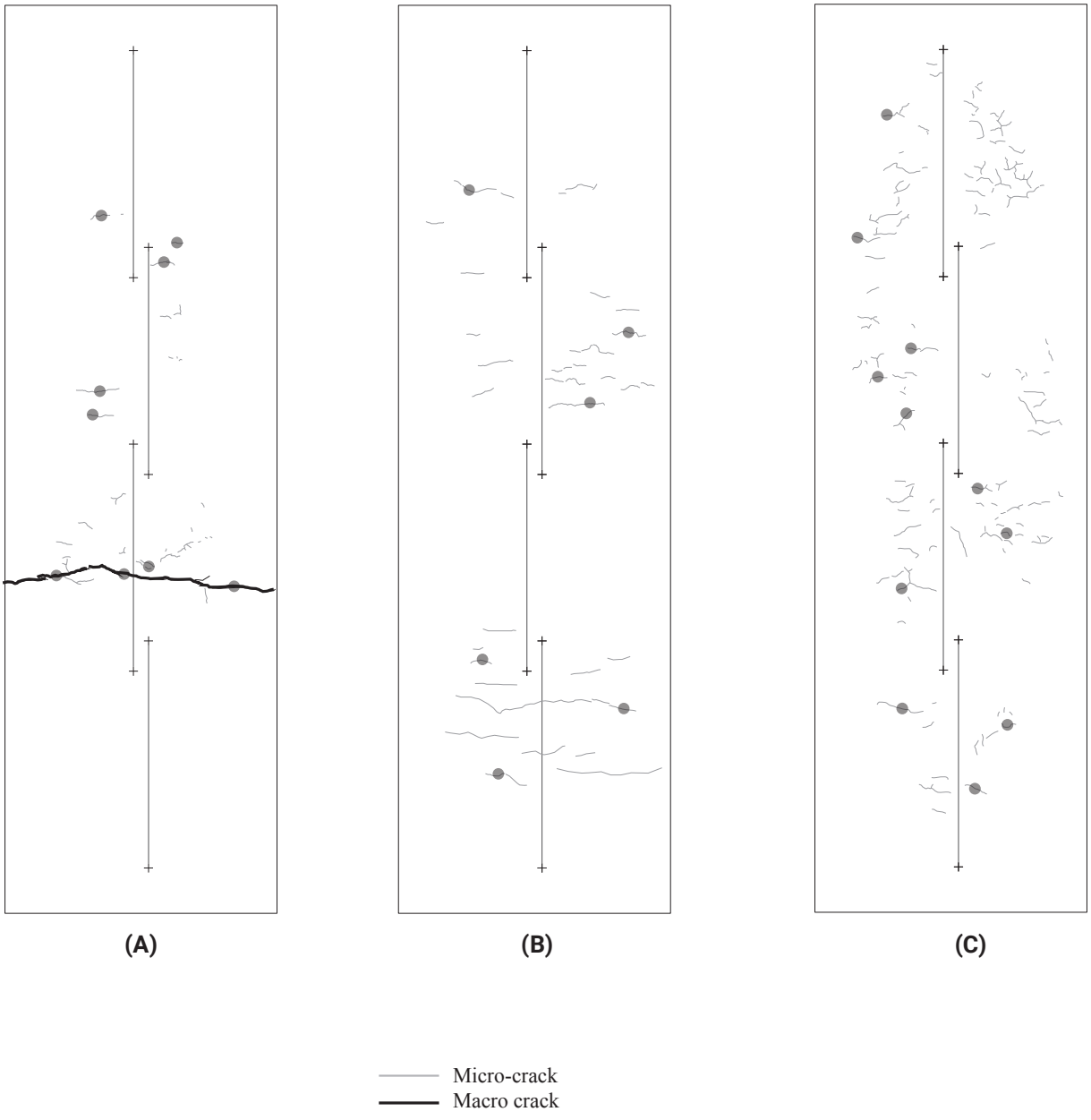

FIGURE 9 – Crack width evolution for each reference crack; a) steel #4 /Φ12, b) fiberglass #4/Φ13, c) fiberglass #3/Φ10

(A)

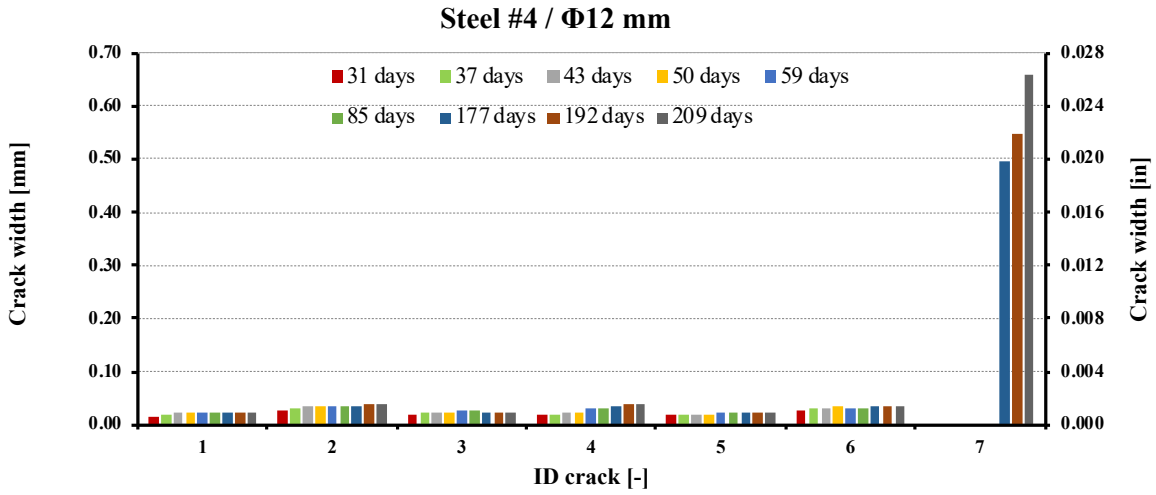

(B)

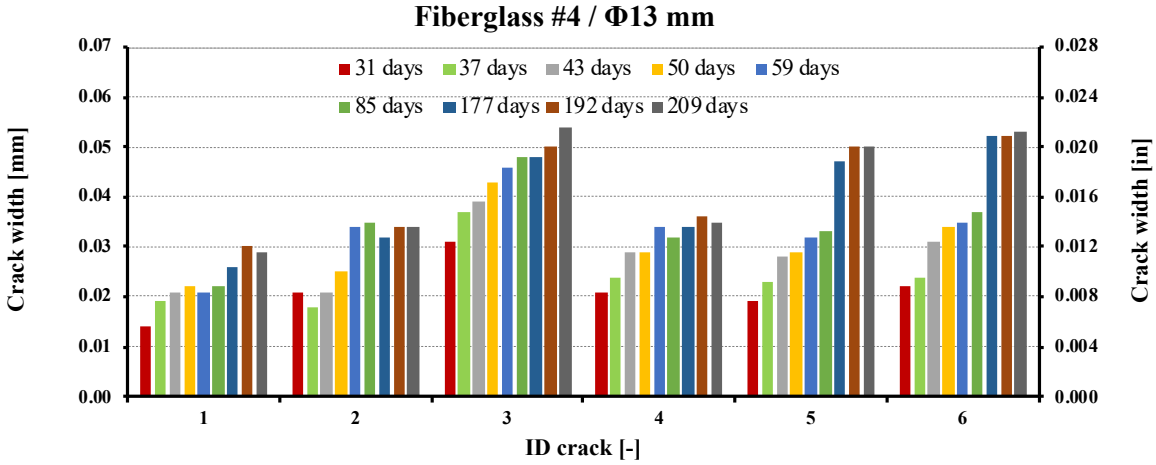

(C)

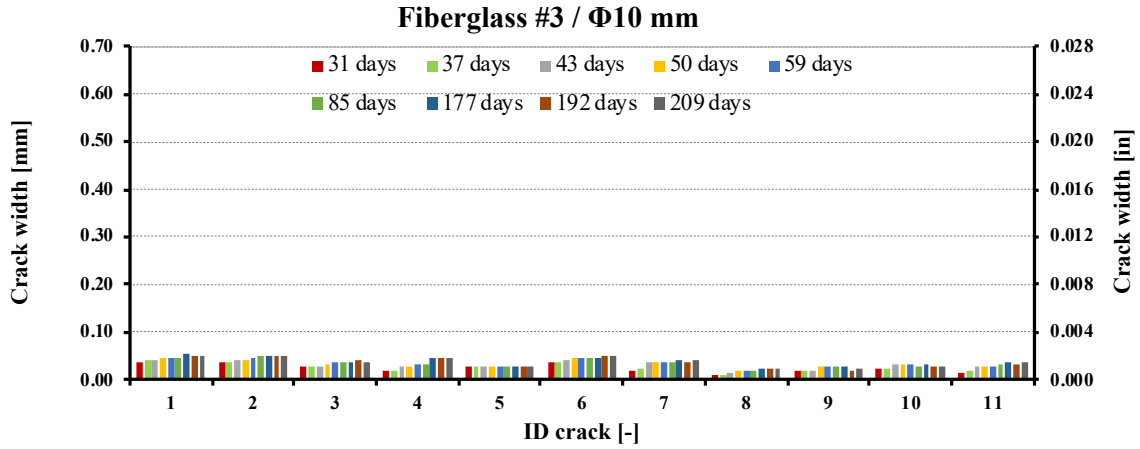

Along the same lines, **Figure 10** plots the maximum crack width observed in each slab vs. time. It can be observed that all slabs exhibit similar trends and crack openings until a macro-crack appears in the slab with steel rebar. As a reference, **Figure 10** also plots the 0.3mm reference level indicating when cracks are actually considered as such in practical terms, i.e. microcracks below 0.3 mm are generally acceptable in floor construction (fib T1.8, 2021).

FIGURE 10 – Maximum crack width vs. time for each slab

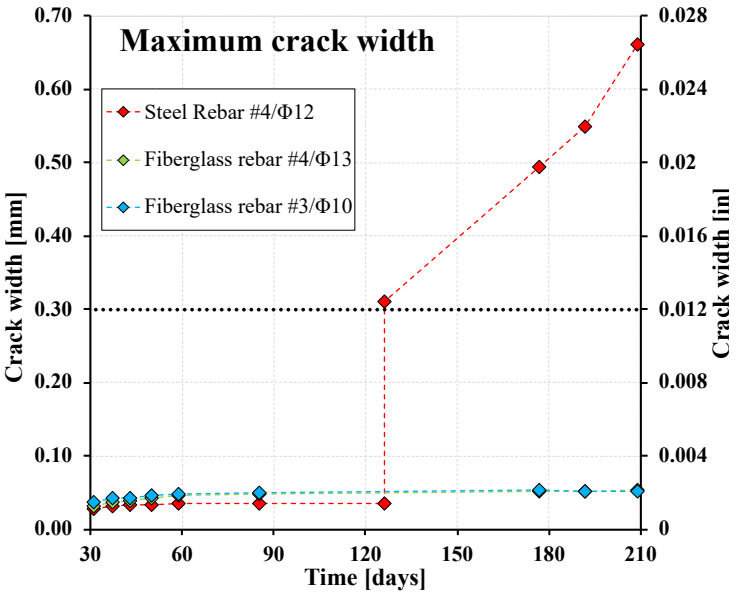

4. CONCLUDING REMARKS

The present paper presents an experimental study proving the effectiveness of fiberglass rebar as shrinkage reinforcement for slabs-on-ground, when compared to a traditional steel rebar solution. Unidimensional slabs reinforced with steel and fiberglass rebars were cast inside steel frames providing high degree of restrain to shrinkage deformations, i.e. providing conditions to favor shrinkage cracking in the elements.

Based on the results and the discussion presented, the following main remarks can be drawn:

1. all slabs show similar crack patterns. As expected, micro-cracks appear in the transversal direction mainly, despite the crazing superficial micro-cracks observed in slabs with #3/10mm fiberglass rebar;
2. all slabs show comparable micro-crack widths;
3. until 90 days from casting, only micro-cracks (width <0.05mm / 0.002 in.) are observed in the three slabs;
4. at 126 days, a macro-crack started developing in the slab reinforced with #4/12 mm steel rebars, presenting a crack width larger than 0.65 mm / 0.025 in. at 209 days;
5. at the same time the number of micro-cracks increased in slabs reinforced with fiberglass, but no localization leading to macro-cracks was observed.

5. ACKNOWLEDGMENTS

The Authors are grateful to Engineer Leporace Guimil Bruno for its valuable support during the experimental activities as well as to the technicians, Augusto Botturi and Andrea Delbarba, for the assistance in performing the experimental program.

6. REFERENCES

[ ] EN 12390-16 (2019). Testing hardened concrete. Part 16: Determination of the shrinkage of concrete. CENTRO DE GESTIÓN: Rue de la Science, 23, B-1040 Brussels, Belgium.

TABLES AND FIGURES

List of Figures:

List of Tables:

APPENDIX

A 1 – Free shrinkage test results

DAYS FROM CASTING	DATE	T	RH	SAMPLE1	SAMPLE2	SAMPLE3	MEAN
[days]	[-]	[°C]	[%]	[μstrain]	[μstrain]	[μstrain]	[μstrain]
3	13/12/2019			0.00	0.00	0.00	0.0
6	16/12/2019			130.26	150.98	186.50	155.9
7	17/12/2019	19.50	45.90	174.66	156.90	278.28	203.3
8	18/12/2019			192.42	171.70	293.08	219.1
9	19/12/2019			216.11	210.19	325.64	250.6
10	20/12/2019			242.75	239.79	396.69	293.1
14	24/12/2019			325.64	304.92	441.10	357.2
23	02/01/2020			476.62	455.90	603.92	512.1
28	07/01/2020	16.80	33.10	452.94	461.82	586.15	500.3
29	08/01/2020	16.80	34.10	449.98	449.98	594.74	498.2
31	10/01/2020	18.80	33.60	503.26	467.74	627.60	532.9
36	15/01/2020	18.00	33.70	518.07	512.14	657.20	562.5
43	22/01/2020	14.70	29.40	544.71	521.03	683.85	583.2
50	29/01/2020	18.90	36.30	553.59	556.55	698.65	602.9
59	07/02/2020	19.00	20.70	592.07	600.96	763.78	652.3
85	04/03/2020	18.80	34.30	615.76	609.84	769.70	665.1

A 2 – Crack width for each crack detected on slab Steel #4 /Φ12, Fiberglass #4 / Φ13, Fiberglass #3 / Φ10s

	TIME	CRACK 1	CRACK 2	CRACK 3	CRACK 4	CRACK 5	CRACK 6	CRACK 7	CRACK 8	CRACK 9	CRACK 10	CRACK 11	MEAN	MAX
	[Days]	[mm]	[mm]	[mm]	[mm]	[mm]	[mm]	[mm]	[mm]	[mm]	[mm]	[mm]	[mm]	[mm]
Steel rebar Φ12@45cm (#4@18")	31	0.016	0.028	0.017	0.018	0.018	0.026	-					**0.021**	**0.028**
	36	0.016	0.033	0.026	0.022	0.018	0.029	-					**0.024**	**0.033**
	37	0.017	0.031	0.021	0.018	0.018	0.032	-					**0.023**	**0.032**
	43	0.021	0.033	0.022	0.021	0.019	0.029	-					**0.024**	**0.033**
	50	0.021	0.034	0.022	0.021	0.019	0.034	-					**0.025**	**0.034**
	59	0.024	0.036	0.026	0.029	0.024	0.031	-					**0.028**	**0.036**
	85	0.024	0.036	0.027	0.029	0.021	0.032	-					**0.028**	**0.036**
	177	0.024	0.036	0.024	0.035	0.022	0.034	0.495					**0.096**	**0.495**
	192	0.024	0.037	0.024	0.038	0.022	0.034	0.549					**0.104**	**0.549**
	209	0.024	0.039	0.021	0.04	0.024	0.034	0.660					**0.120**	**0.660**
Fiberglass rebar Φ13@45cm (#4@18")	31	0.014	0.021	0.031	0.021	0.019	0.022						**0.021**	**0.031**
	36	0.02	0.021	0.036	0.024	0.028	0.022						**0.025**	**0.036**
	37	0.019	0.018	0.037	0.024	0.023	0.024						**0.024**	**0.037**
	43	0.021	0.021	0.039	0.029	0.028	0.031						**0.028**	**0.039**
	50	0.022	0.025	0.043	0.029	0.029	0.034						**0.030**	**0.043**
	59	0.021	0.034	0.046	0.034	0.032	0.035						**0.034**	**0.046**
	85	0.022	0.035	0.048	0.032	0.033	0.037						**0.035**	**0.048**
	177	0.026	0.032	0.048	0.034	0.047	0.052						**0.040**	**0.052**
	192	0.03	0.034	0.05	0.036	0.05	0.052						**0.042**	**0.052**
	209	0.029	0.034	0.054	0.035	0.05	0.053						**0.043**	**0.054**
Fiberglass rebar Φ10@45cm (#3@18")	31	0.035	0.035	0.028	0.018	0.026	0.037	0.018	0.012	0.018	0.022	0.013	**0.024**	**0.037**
	36	0.04	0.041	0.027	0.022	0.026	0.039	0.03	0.014	0.025	0.026	0.023	**0.028**	**0.041**
	37	0.042	0.036	0.028	0.018	0.027	0.039	0.025	0.012	0.018	0.022	0.021	**0.026**	**0.042**
	43	0.042	0.04	0.03	0.027	0.03	0.043	0.037	0.017	0.021	0.031	0.026	**0.031**	**0.043**
	50	0.047	0.042	0.034	0.029	0.03	0.045	0.037	0.019	0.028	0.031	0.029	**0.034**	**0.047**
	59	0.048	0.046	0.039	0.031	0.027	0.044	0.037	0.019	0.029	0.031	0.029	**0.035**	**0.048**
	85	0.048	0.05	0.036	0.032	0.027	0.045	0.037	0.019	0.03	0.026	0.031	**0.035**	**0.050**
	177	0.053	0.049	0.036	0.046	0.03	0.048	0.042	0.022	0.028	0.031	0.039	**0.039**	**0.053**
	192	0.05	0.049	0.04	0.045	0.029	0.051	0.039	0.023	0.021	0.029	0.033	**0.037**	**0.051**
	209	0.052	0.049	0.038	0.046	0.029	0.052	0.041	0.024	0.024	0.029	0.036	**0.038**	**0.052**

HOW WE BUILD NOW™

INFRASTRUCTURE SOLUTIONS

Owens Corning Infrastructure Solutions, LLC.
One Owens Corning Parkway
Toledo, OH, 43659 USA
1-855-OC-Rebar

https://www.owenscorning.com/rebar